Materials Transactions, Vol. 50, No. 5 (2009) pp. 940 to 942
Special Issue on Nano-Materials Science for Atomic Scale Modification

Simultaneous Atomic Imaging of Atomic Force Microscopy and Scanning Tunneling Microscopy Using Metal Coated Cantilevers

Daisuke Sawada[1], Akira Hirai[1], Yoshiaki Sugimoto[1], Masayuki Abe[1,2,*] and Seizo Morita[1]

[1]*Graduate School of Engineering, Osaka University, Suita 565-0871, Japan*
[2]*PRESTO, Japan Science and Technology Agency, Kawaguchi 332-0012, Japan*

Imaging of surface atoms with simultaneous measurement of noncontact atomic force microscopy (NC-AFM) and scanning tunneling microscopy (STM) is performed. Si cantilever coated with PtIr provides stable AFM/STM operations to obtain high spatial resolution images. AFM/STM measurements on Si(111)-(7×7), Ge(111)-c(2×8), and TiO_2(110) surfaces are presented at room temperature. On the Ge(111)-c(2×8) surface, adatom and restatom sites which have the same atomic patterns are determined from dual bias AFM/STM measurements.
[doi:10.2320/matertrans.MC200818]

(Received November 4, 2008; Accepted January 16, 2009; Published March 11, 2009)

Keywords: *atomic force microscopy, scanning tunneling microscopy, frequency modulation, TiO_2, Si(111), Ge(111)*

1. Introduction

Characterization of materials in an atomic level is crucial to advance the fields of nanoscience and nanotechnology. Surface imaging by scanning probe microscopy (SPM) is a conventional method for seeing the characters of materials and/or electronic devices. Among various types of SPM techniques, scanning tunneling microscopy (STM) and noncontact atomic force microscopy (NC-AFM)[1)] have been used in imaging surface atoms. Although both methods allow us to obtain atomic resolution images, the measurement quantities are different. Tunneling current detected in STM correspond to local density of state of the electronic charges of surface. NC-AFM can image surface topography.[2)] In order to understand material properties in atomic level, simultaneous measurement of the tunneling current and atomic force is required. To date, various AFM/STM measurements have been done using silicon[3–5)] and metal[6–8)] tips. Although we can expect high resolution images using the Si cantilevers, interpretation of the image contrast in STM becomes more complicated. This is because obtained tunneling current includes both property of the tip and sample.

In this paper, authors demonstrate simultaneous AFM/STM measurements with high spatial resolution on various surface systems. In order to improve the quality of the simultaneous imaging, we have employed Si cantilever coated with PtIr film. For imaging the surface using atomic force, it is preferable to detect large interaction force for improvement of signal to noise ratio. Because of the metallic property, it is thought that interaction force between atoms of PtIr tip apex and sample surface is different from the case of Si cantilever. But our expectation is that the PtIr tip picks up Si atoms at the apex itself during scan. This enabled us to detect force and tunneling current simultaneously. The same mechanism has already been discussed in the case of the NC-AFM measurements on ionic crystals. One obtains atomic resolution image of the ionic surface after the AFM apex picks up the cations or anions during scan. When the apex atom is the cations (anions), surface anions (cations) would be imaged as bright spots.

*Corresponding author, E-mail: abe@eei.eng.osaka-u.ac.jp

2. Experimental

We used a home-built NC-AFM operated at room temperature (RT) and ultra-high vacuum (UHV). The base pressure was less than 1×10^{-8} Pa. The cantilever displacement was detected by an optical interferometer. Si cantilevers which were coated by PtIr and cleaned up by Ar ion sputtering were used in the constant amplitude mode. Usually tungsten tip is used for STM measurements. In our case, to reduce the oxidation of the tip apex, we have selected PtIr coat AFM tip. In order to perform the simultaneous image acquisition, we have controlled the tip-sample distance by keeping the Δf constant and obtained AFM topographic images. During the scan, we measured tunneling currents and imaged them as STM measurement at the same time.

3. Results and Discussions

Using the PtIr AFM tip, we have performed AFM/STM measurements on Si(111)-(7×7) surface. We have prepared the Si(111)-(7×7) surface in UHV by degassing at 600°C for a few days, flashing at 1200°C, and cooling down slowly from 900°C to RT. We cleaned the PtIr AFM tip by Ar ion sputtering, and introduce it to the AFM observation chamber *in-situ*. Figure 1 show images of the AFM/STM simultaneous measurement on the Si(111)-(7×7) surface. Images of AFM (Fig. 1(a)) and STM (Fig. 1(b)) were obtained simultaneously at $Vs = 400$ mV. In the same way, we have performed simultaneous AFM/STM measurement at negative bias voltage ($Vs = -500$ mV) as in Fig. 1(c) and (d) of AFM topographic and STM images, respectively. In the both positive and negative bias voltages, single atoms are clearly imaged. Contrast difference between the faulted and the unfaulted halves in Fig. 1(d) means that tip condition was preferable for STM measurement.

Usefulness of the AFM/STM measurements is increased when one studies some relations between topographic and electronic properties of surface system. As an example, we applied the simultaneous AFM/STM measurement on Ge(111)-c(2×8) surface in which the surface structures for the adatoms and the restatoms were the same. In our previous study, we have found that on this surface, there are two types

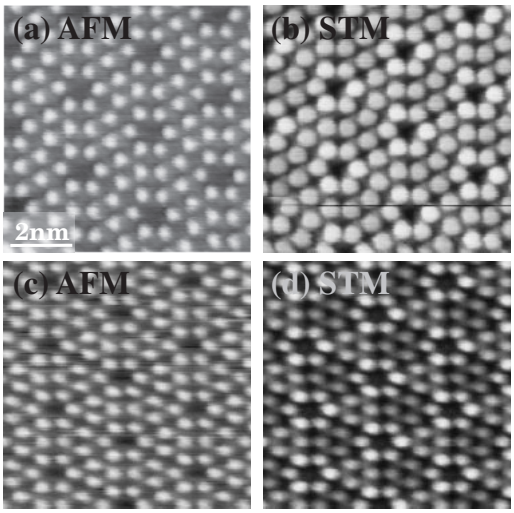

Fig. 1 Images of simultaneous AFM/STM measurements on the Si(111)-(7×7). AFM topographic image by keeping the frequency shift Δf constant was acquired with the tunneling current at the same time during the scan. In Figs. (a) and (b) ((c) and (d)) obtained simultaneously, Vs = 400 mV (−500 mV) sample bias voltage was applied. PtIr coated silicon cantilevers were used. Respective experimental parameters of the cantilever oscillation amplitude, free-oscillation first mechanical resonance frequency, and spring constant were $A = 30$ nm, $f_r = 284093$ Hz, and $k = 22.9\,\mathrm{Nm^{-1}}$ for Figs. (a) and (b), and $A = 17.4$ nm, $f_r = 289139$ Hz, and $k = 26.9\,\mathrm{Nm^{-1}}$ for Figs. (c) and (d).

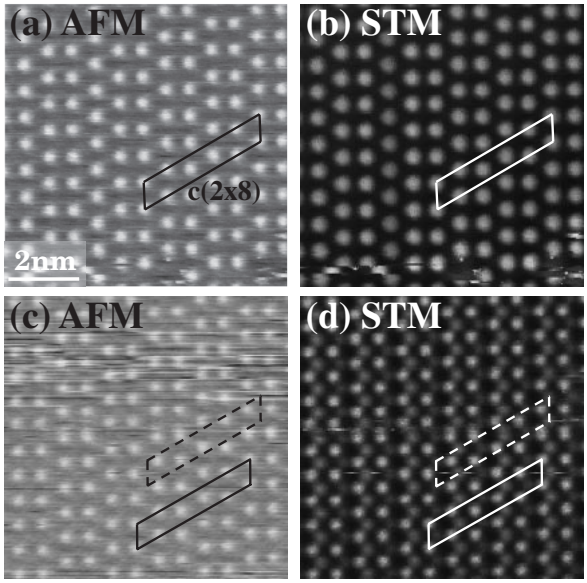

Fig. 2 Images by AFM/STM simultaneous measurements on the Ge(111)-c(2×8). In Figs. (a) and (b) ((c) and (d)) obtained simultaneously, Vs = 500 mV (−500 mV) sample bias voltage was applied. PtIr coated silicon cantilevers were used. Respective experimental parameters of the cantilever oscillation amplitude, free-oscillation first mechanical resonance frequency, and spring constant were $A = 15.2$ nm, $f_r = 278819$ Hz, and $k = 21.7$ N/m for Figs. (a) and (b), and $A = 14.6$ nm, $f_r = 311353$ Hz, and $k = 33.6$ N/m for Figs. (c) and (d). c(2×8) unit cells are put on both AFM and STM images at the same places based on the adatoms (solid line) and the restatoms (dashed line) in the STM image.

of topographic contrast images depending on the tip apex structure and/or composition.[9] In one of them only the adatoms are imaged, while in the other both the adatom and the restatom are imaged. In some of the images in the latter case, the distinction between adatoms and restatoms is unclear due to a special configuration and/or composition of the tip apex. In NC-AFM images, it is generally thought that structural height difference would necessarily manifest itself in a difference of image contrast when images are acquired at small frequency shift values.[2] Due to the same pattern of the adatoms and the restatoms, it is difficult to judge the atomic sites only from the AFM information. Moreover, the fact that the difference in the electronic occupancy of the dangling bonds of both the adatoms and the restatoms of the Ge(111)-c(2×8) surface[10] could affect the interaction force complicates the imaging mechanism in NC-AFM. In order to discriminate the atoms in the Ge(111)-c(2×8) image, we had needed to evaporate a small number of Sn atoms in our previous study.[9] Sn atoms embedded in the adatom site of Ge(111)-c(2×8) surface, which enabled us to interpret the image contrast of the Ge(111)-c(2×8) surface. In STM measurements on the Ge(111)-c(2×8) surface, on the other hand, the dual-polarity bias image acquisition method provides both empty and filled state images of the surface. It is possible to clarify the position of both the adatoms and restatoms.[11–13] In particular, in the filled state image acquired at sample bias voltage of −2 V, the partial charge transfer from the adatom to the restatom of the Ge(111)-c(2×8) surface provides images with the restatoms enhanced over the adatoms.[13]

In Fig. 2, we have performed the AFM/STM simultaneous measurement on the Ge(111)-c(2×8) surface at bias voltages of Vs = 500 mV for Fig. 2(a) and (b) and of Vs = −500 mV for Figs. 2(c) and (d), respectively. Clean Ge(111)-c(2×8) reconstructed surfaces were obtained by successive Ar ion sputtering and annealing of a commercial Ge(111) wafer. Unit cells of the c(2×8) are drawn in synchronization with atomic sites. In the empty state STM image of Fig. 2(b), bright atomic spots correspond to the adatom sites.[13] This means that adatoms are imaged in NC-AFM measurement with this PtIr tip from the comparison of the position of the c(2×8) unit cells. The filled state STM image of Fig. 2(d) shows two atomic patterns. Bright and dim spots are adatoms and restatoms, respectively.[13] We have put the c(2×8) unit cells on both AFM and STM images at the same places based on the adatoms (solid line) and the restatoms (dashed line) in the STM image. Comparing the positions of the c(2×8) cells, atoms imaged in the AFM are adatoms with this typical PtIr tip.

We have applied the AFM/STM measurement using PtIr tips on the TiO_2(110) surface, one of the metal oxides that has attracted much interest over decades. Also on this surface, the PtIr AFM tip allowed us to image atomic force and tunneling current at the same time as in Fig. 3. We obtained clean TiO_2(110) surfaces by successive Ar ion sputtering and annealing. Comparing to previous study,[14] bright spot in STM image of Fig. 3(b) would be titanium. Bright contrast was also in the AFM image of Fig. 3(a) at the same rows, titanium atoms were imaged as bright spots. But we need to be careful for imaging mechanism because we have also found AFM image contrast depended on the material properties of the tip apex (data not shown). We also have confirmed that vacancy sites (circles in Fig. 3) in both AFM and STM images.

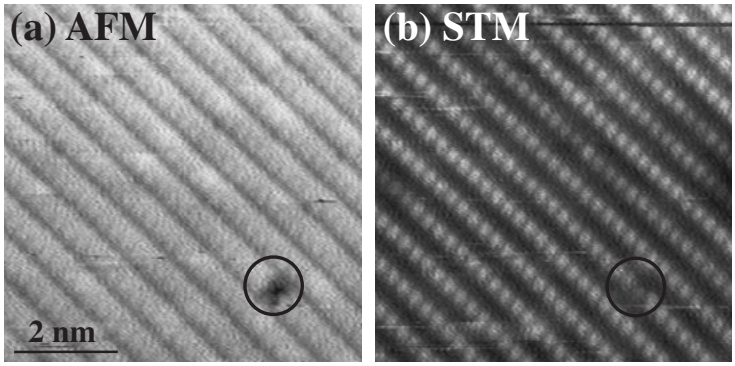

Fig. 3 AFM/SIM images on Ti(110)-(1×1) surface. Simultaneous imaging was performed using a silicon tip coated with PtIr. Sample bias voltage was Vs = 1000 mV. Oscillation amplitude, free-oscillation first mechanical resonance frequency, and spring constant of the cantilever were $A = 16.6$ nm, $f_r = 306611$ Hz, and $k = 28.6$ N/m.

Although we have found appropriate tip condition for the AFM/STM simultaneous measurements, there remain some issues for reliable data acquisition about imaging mode. In this paper, for tip-sample distance regulation, we used the feedback with atomic force by keeping the frequency shift constant during scan. In almost all previous study, feedback with AFM or STM was used. This might cause signal crosstalk between AFM and STM even when experimental parameters are set carefully. In order to reduce the crosstalk problem, constant height AFM/STM in which no feedback is activated should be employed and frequency shift and tunneling current should be detected simultaneously during scan. This mode requires the condition that movement of the tip-sample position is negligible. With conventional setup of AFM and/or STM experiments, however, relative tip-sample position always change due to the thermal drift, especially at RT. As one of the method for tip-sample control, compensation of the thermal drift using the atom-tracking[15,16] and the feedforward[17] techniques are useful. Atom manipulation,[18–20] atom identification,[21] and force mapping[22] at RT in which precise tip-sample positioning is need have been successfully demonstrated using these techniques. We expect the application of the precise tip-sample positioning to the appropriate AFM/STM measurements.[23]

In summary, we have performed simultaneous measurement of noncontact atomic force microscopy and scanning tunneling microscopy at room temperature and ultra-high vacuum. Si cantilever coated with PtIr enabled us to perform stable simultaneous imaging. On the Ge(111)-c(2×8) surface, dual bias measurement was performed in order to discriminate adatoms and restatoms. We also succeeded in imaging TiO_2(110) surface with the AFM/STM simultaneous measurement.

Acknowledgement

This work was supported by the Grant-in-Aid for Scientific Research (No. 19053006, No. 17101003, No. 18860046, No. 20760024, and No. 19360017) from the Ministry of Education, Culture, Sports, Science and Technology of Japan (MEXT), Japan Science and Technology Agency (JST), Frontier Research Center in Osaka University, the project Atomic Technology and the Global Center of Excellence programs funded by MEXT. The work of Y.S. is supported by The Frontier Research Base for Global Young Researchers, Osaka University, on the Program of Promotion of Environmental Improvement to Enhance Young Researchers' Independence under the Special Coordination Funds for Promoting Science and Technology of MEXT.

REFERENCES

1) S. Morita, R. Wiesendanger and E. Meyer: *Noncontact Atomic Force Microscopy* (Berlin, Springer, 2002).
2) Y. Sugimoto, P. Pou, O. Custance, P. Jelinek, S. Morita, R. Pérez and M. Abe: Phys. Rev. B **73** (2006) 205329.
3) P. Güthner: J. Vac. Sci. Technol. B **14** (1996) 2428.
4) T. Arai and M. Tomitori: Phys. Rev. Lett. **93** (2004) 256101.
5) G. H. Enevoldsen, H. P. Pinto, A. S. Foster, M. C. R. Jensen, A. Kühnle, M. Reichling, W. A. Hofer, J. V. Lauritsen and F. Besenbacher: Phys. Rev. B **78** (2008) 045416.
6) A. Oral, R. A. Grimble, H. O. Özer, P. M. Hoffmann and J. B. Pethica: Appl. Phys. Lett. **79** (2001) 1915.
7) S. Hembacher, F. J. Giessibl, J. Mannhart and C. F. Quate: Proc. Natl. Acad. Sci. **100** (2003) 12539.
8) M. Ternes, C. P. Luts, C. F. Hirjibehedin, F. J. Giessibl and A. J. Heinrich: Science **319** (2008) 1066.
9) M. Abe, Y. Sugimoto and S. Morita: Nanotechnol. **16** (2005) S68.
10) R. S. Becker, B. S. Swartzentruber, J. S. Vickers and T. Klitsner: Phys. Rev. B **39** (1989) 1633.
11) E. S. Hirschorn, D. S. Lin, F. M. Leibsle, A. Samsavar and T.-C. Chiang: Phys. Rev. B **44** (1991) 1403.
12) P. Molin'as-Mata and J. Zegenhagen: Phys. Rev. B **47** (1993) 10319.
13) G. Lee, H. Mai, I. Chizhov and R. F. Willis: J. Vac. Sci. Technol. A **16** (1998) 1006.
14) G. H. Enevoldesen, A. S. Foster, M. C. Christensen, J. V. Lauritsen and F. Besenbacher: Phys. Rev. B **76** (2007) 205415.
15) M. Abe, Y. Sugimoto, O. Custance and S. Morita: Appl. Phys. Lett. **87** (2005) 173503.
16) M. Abe, Y. Sugimoto, O. Custance and S. Morita: Nanotechnol. **16** (2005) 3029.
17) M. Abe, Y. Sugimoto, T. Namikawa, K. Morita, N. Oyabu and S. Morita: Appl. Phys. Lett. **90** (2007) 203103.
18) Y. Sugimoto, M. Abe, S. Hirayama, N. Oyabu, O. Custance and S. Morita: Nature Mater. **4** (2005) 156.
19) Y. Sugimoto, P. Jelinek, P. Pou, M. Abe, S. Morita, R. Perez and O. Custance: Phys. Rev. Lett. **98** (2007) 106104.
20) Y. Sugimoto, P. Pou, O. Custance, P. Jelinek, M. Abe, R. Perez and S. Morita: Science **322** (2008) 413.
21) Y. Sugimoto, P. Pou, M. Abe, P. Jelinek, R. Perez, S. Morita and O. Custance: Nature (London) **446** (2007) 64.
22) Y. Sugimoto, T. Namikawa, K. Miki, M. Abe and S. Morita: Phys. Rev. B **77** (2008) 195424.
23) D. Sawada, Y. Sugimoto, M. Abe and S. Morita: *in preparation.*